COBEM UBERLÂNDIA 2019

ABCM Associação Brasileira de Engenharia e Ciências Mecânicas

25th ABCM International Congress of Mechanical Engineering
October 20-25, 2019, Uberlândia, MG, Brazil

COB-2019-1406
THE INFLUENCE OF AIR-SOLID FUEL RATE IN COMBUSTION PROCESS USING CFD

Fábio da Silva Barros
Pedro Oliveira Carvalho da Silva
Danielle Regina da Silva Guerra
Rodrigo Cavalcanti Ribeiro Lima
L.F.R. Castelo Branco
Universidade Federal do Pará, Rua Augusto Corrêa, 01 - Guamá
fabiobaarros@gmail.com
pedro.0106@gmail.com
daguerra@ufpa.br
rodrigo.c.ribeiro@hotmail.com
leticia.branco@maraba.ufpa.br

Abstract. *In recent years many researchers have developed different numerical models to predict and optimize the combustion process. To develop such models is necessary to know the oxidation reactions and heat transfer between the combustion products and the wall of the chamber, which requires analysis of chemical kinetic mechanisms, flow behavior and heat transfer. The aim of this work is to analyze computationally, through Ansys Fluent comercial code, a cyclonic furnace for biomass burning, changing the air-fuel ratio to improve the operating conditions of the equipment. The multiphase flow was solved using Euler-Lagrange model, with the particles being treated as dispersed phase and their trajectories computed by Lagrange equations. For the gas phase reaction, the model used was the Finite-Rate / Eddy-Dissipation, where a two-step reaction was assumed. The $\kappa-\epsilon$ RNG model was used for turbulence because it shown a good concordance in cyclonic behavior and has a relatively low computational cost. The radiation effect was solved using the P1 approach method. With the results obtained it was possible to identify the region where the combustion occurs, the fields of velocity, temperature, concentrations of the chemical species, emission of exhaust gases and compare each equivalence ratio showing its main characteristics and their effects in combustion process.*

Keywords: *Combustion, Biomass, Cyclonic furnace, Reactive Flows.*

1. INTRODUCTION

The combustion reactions are present in several production of manufacturing processes and also on energy generation, as thermal, mechanical or electric energy. The modeling of the combustion process is linked to some interests such as: productive efficiency, financial, reduction of production costs, and from the environmental point of view, reducing greenhouse gas emissions.

The production of steam through the burning of a fuel has been shown to be very important by the alternative energy generation, so that understanding the combustion reaction is important. An efficient combustion operation depends on the knowledge of the oxidation reactions, the heat transfer between the combustion products and the chamber walls, which requires a detailed analysis of the reaction mechanisms and the flow behavior.

The world's energy matrix is mostly made up of fossil fuels, mainly petroleum, coal and natural gas, the sector that contributes most to global warming and is responsible for the emission of 76% of greenhouse gases in 2017, in the world (IEA, 2018).

With the growing concern about the environmental damage caused by these energy sources, it is necessary to search for new fuels that are less harmful to the environment. Biomass is one of the energy sources with the greatest growth potential in recent years, being considered as one of the main alternative for the diversification of the energy matrix and the consequent reduction of dependence on fossil fuels.

Biomass as fuel has as its most important feature a porous structure and its elemental chemical composition, basically composed of carbon and oxygen, which combine to form molecular chains that make up the biomass: cellulose, hemicellulose and lignin, Tillman (1991).

Vasconcelos (2008) proposed a combustion analysis in a cyclonic chamber, and experimental measurements of temperature and gas concentration in the internal wall of the combustion chamber. In this study, parameters such as air-sawing

were varied in poor equivalence ratios, with excess air. The experimental data were computed and compared with results found numerically by Cunha (2005) using Fluent software. Vasconcelos (2008) identified the minimum operational equivalence ratio for the cyclonic chamber to have low levels of pollutants in its gaseous products.

Entering into the computational simulation, Silva (2007) proposed the simulation of combustion of unpremixed natural gas in an axissimetric cyclonic chamber, focusing the effects of thermal radiation on the temperature and chemical species concentration fields, also the heat transfer analyses. The thermal radiation in the combustion chamber is based on the zonal method, which consists in dividing the computational domain into finite-size zones in the gas and in the surfaces, the effect of the wavelength dependence of the gas absorption coefficient through of the greenhouse gas-weighted mass model (WSGGM).

Guessab (2013) made flame simulations without pre-mixing of methane and air, using the RANS model for turbulence and the Finite-Rate / Eddy-Disssipation hybrid model for the reaction. The results of the simulation were compared between the global reaction mechanism and a simplified four-step mechanism, the latter presenting higher flame length, reaction heat and adiabatic flame temperature below the values established in the global reaction simulation due to the presence of CO and H_2 O in the reaction products.

Sun (2015) presentes a three-dimensional numerical simulation to study the pulverized-coal combustion process in a tangentially fired ultra-supercritical boiler. In this study the realizable k-e model was used for gas coupled with discrete phase model for coal particles, P-1 radiation model for radiation, two-competing-rates model for devolatilization, and kinetics/diffusion-limited model for combustion process are considered. The characteristics of the flow field, particle motion, temperature distribution, species components, and NOx emissions were numerically investigated.

Silva (2019) uses a commercial CFD code, CFX Ansys Ltd., to study the pulverized-coal combustion process in a 160 MWe thermal power plant erected in the core of the Brazilian coal reserves region, with the objective of simulating the operation conditions and identifying inefficiency factors. The behavior of the flow of air and pulverized coal through the burners was analyzed, and the three-dimensional flue gas flow through the combustion chamber and heat exchangers was reproduced in the numeric simulation.

Lima (2016) investigated computationally the combustion process in a cyclonic furnace, where models of reaction, phase coupling, turbulence, radiation and discrete phase are described. Results of temperature fields, velocity vectors and NOx pollutant formation are analyzed according to literature - based data and experimental data from the cyclonic boiler.

The objective in the present work is to compare CFD analysis between different air-fuel ratios in a cyclonic furnace proposed by Lima (2016), so that a more efficient boiler operation condition can be defined.

2. THEORETICAL FOUNDATION

2.1 Cyclonic chamber

Cyclonic chamber is basically a cylindrical chamber where the particulate solid fuel burns in a cyclonic motion due to the air that is introduced tangentially to the chamber.

The cyclonic chamber equipment used as the basis for this work is located in the mechanical engineering laboratory of the UFPA, developed by the research group EBMA from a research project. This boiler is characterized as a mixed boiler, where in its upper part it has a flamotubular boiler and a furnace covered by a wall of water.

Wood sawdust and air are insulated to the furnace pre-mixed in the tangent direction following the contour through the walls to exit. The actual feed system has some limitations such as obstruction the feed screw and deregulating the load cells.

Immediately after passing through the furnace, the produced gases from the burning enter the upper tank of the furnace by tubes, exchanging heat with the water and passing through a cyclonic separator for removal the particles from the combustion.

In this type of configuration the reactions occur close to the wall, since the difference between the density of the reactants causes the solid sawdust particles to be drawn into the chamber wall as the air is drawn into the cylinder by the centrifugal force of the flow. With the reactions located on the wall, it is evident that the highest temperatures will be in this region.

3. COMPUTATIONAL MODELING

The numerical simulations developed in this work were obtained from the Ansys Fluent commercial code. This code solves the problems using the finite volume method, where the physical system is discretized in smaller control volumes, generating the mesh, so that the differential equations are replaced by algebraic equations.

3.1 Geometry and mesh

The chamber geometry was constructed based on the real chamber, which consists of its first part in a cylindrical tube of 0.6m in diameter by 2m in length, followed by a gas outlet zone with radius of curvature 0.8m and outlet diameter 0.3m. The air intake is made by a feeder of dimensions 0.05m by 0.05m.

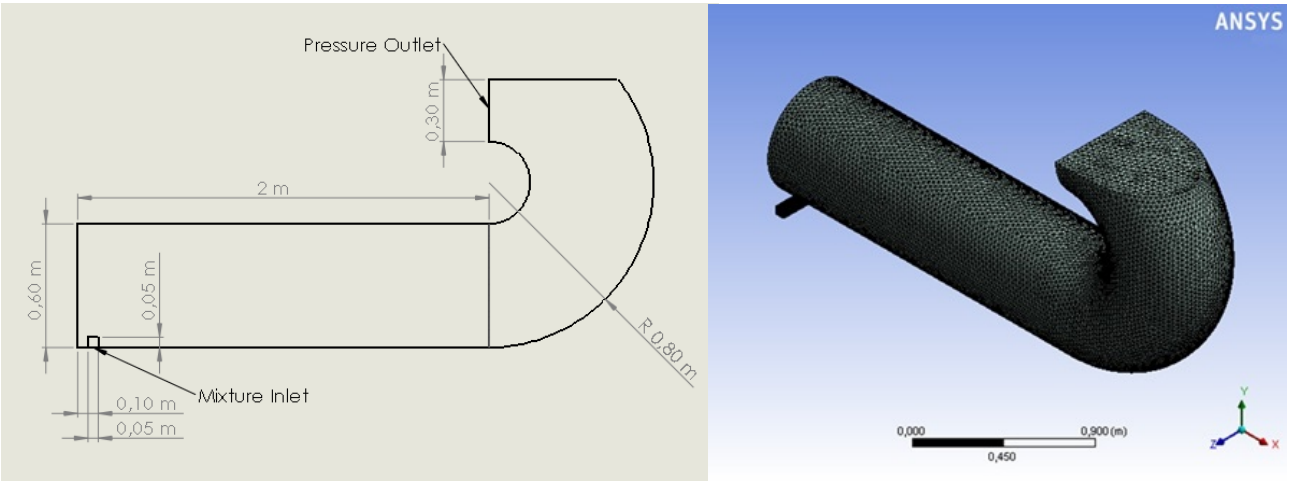

(a) Geometry dimensions (b) Mesh

Figure 1: Domain characteristics.

The development of the computational mesh has a direct influence on the precision of the problem solution, so to develop a mesh that has good agreement with the calculation domains is extremely important. Here the non - structured, tetrahedral 3D mesh, with 61,550 nodes and 325,286 elements, was constructed.

3.2 Numerical Modeling

To solve the problem of dispersed multiphase flows the Ansys Fluent computational tool has two approaches: Eulerian-Lagrangian and Eulerian-Eulerian. Since it is necessary an accurately estimative of the particles trajectory, the Euler-Lagrange approach was chosen. For this work, the one-way coupling model was used, which describes the behavior of the discrete phase based on a continuous flow field of the continuous phase. To model a combustion process, it is necessary to take into account many factors. The Fluent package provides several tools to facilitate the numerical modelling, such as turbulence models, radiation models, discrete phase model and reaction models. This section will briefly describe the models used in this simulation.

3.2.1 Turbulence model

The Navier-Stokes equation are analytically unsolvable for most real flows, and also present a obstacle when a numerical method is used. This obstacle is known as the closure problem. Turbulence models were developed with the purpose of modeling the Reynolds stress tensor that arises when the Navier-Stokes equations become the RANS (Reynolds-Averaged Navier-Stokes). The combustion process at hand is characterized by a cyclonic flow, and due to this factor the RNG $k-\epsilon$ turbulence model was chosen. This model is a refinement of the standard $k-\epsilon$ model, and is obtained via a technique called Re-normalization Group Theory (RNG). The equations for k and ϵ are the following:

$$\frac{\partial \rho k}{\partial t} + \nabla\left(\rho k u_i\right) = \nabla\left(\alpha_k \mu_{eff} \nabla k\right) + G_k + G_b - \rho\epsilon - Y_M + S_k \tag{1}$$

$$\frac{\partial \rho \epsilon}{\partial t} + \nabla\left(\rho \epsilon u_i\right) = \nabla\left(\alpha_k \mu_{eff} \nabla \epsilon\right) + C_{1\epsilon}\frac{\epsilon}{k}\left(G_k + C_{3\epsilon} G_b\right) - C_{2\epsilon}\rho\frac{\epsilon^2}{k} - R_\epsilon + S_\epsilon \tag{2}$$

$$\mu_t = \rho C_\mu \frac{k^2}{\epsilon} \tag{3}$$

Where μ_{eff} is the effective viscosity, R_ϵ is a new term derived from the RNG theory. C_μ, $C_{1\epsilon}$ and $C_{2\epsilon}$ are 0.0845, 1.42 and 1.68, respectively. S_k and S_ϵ are predefined source terms. α_k and α_ϵ are the inverse of the effective Prandtl number for k and ϵ.

3.2.2 Force balancing on particle

Using the Eulerian-Lagrangean approach, the particle trajectory can be calculated via integration of the forces balance acting on the particle.

$$\frac{du_p}{dt} = F_D\left(\vec{u} - \vec{u}_p\right) + \frac{\vec{g}\left(\rho_p - \rho\right)}{\rho_p} \tag{4}$$

Where the term $F_D\left(\vec{u} - \vec{u}_p\right)$ is the drag force per unit of particle mass.

$$F_D = \frac{18\mu C_D Re}{\rho_p d_p^2 24} \tag{5}$$

The drag coefficient of the particles is modeled by a non-spherical drag law proposed by Haider & Levenspiel, as shown by eq. 6

$$C_D = \frac{24}{Re_{sph}}(1 + b_1 Re_{sph}^{b_2}) + \frac{b_3 Re_{sph}}{b_4 + Re_{sph}} \tag{6}$$

3.2.3 Gaseous combustion reaction model

For the reaction modeling, the species transport model with volumetric reactions was chosen. However, in biomass combustion, there are reactions that occur in the gas phase as well as the solid phase. For the gaseous reactions, a finite-rate/eddy-dissipation model was selected.In the finite-rate / eddy-dissipation model, the net reaction rate is taken as the minimum between the rate calculated by the Arrhenius equation and the viscous dissipation equation. In practice, the Arrhenius rate acts as a "switch" to chemical kinetics, preventing the reaction from occurring before the flame front. Since ignition occurs, the viscous dissipation rate is generally lower than the Arrhenius rate, and the reaction is limited by mixing. In order to determine the reaction rate, the model calculates the rate using the Arrhenius equation and the eddy dissipation equation, using the smaller of the two. Eq. 7 describes the finite rate equation.

$$R_{i,r} = k_{f,r} \prod_{j=1}^{N} [C_{j,r}]^{\left(n_{j,r}^{'} + n_{j,r}^{"}\right)} \tag{7}$$

Where $k_{f,r}$ is given by:

$$k_{f,r} = A_r T^{\beta_r} e^{\frac{-E_r}{R_u T}} \tag{8}$$

In the Eddy Dissipation model, the net rate is obtained by using the following two equations:

$$R_{i,r} = v_{i,r}^{'} M_{w,i} A \rho \frac{\epsilon}{k} min\Re\left(\frac{Y_\Re}{v_{\Re,r}^{'} M_{w,\Re}}\right) \tag{9}$$

$$R_{i,r} = v_{i,r}^{'} M_{w,i} A B \rho \frac{\epsilon}{k} \frac{\sum_P Y_P}{\sum_j^N v_{j,r}^{"} M_{w,j}} \tag{10}$$

3.2.4 Heterogeneous particle combustion

The heat balance for the solid phase is given by Eq. 11:

$$m_P C_P \frac{dT_P}{dt} = hA_P\left(T_\infty - T_P\right) + \epsilon_P A_P \sigma\left(\theta_R^4 - T_P^4\right) \tag{11}$$

Where m_P is the particle mass, c_P is the specific heat at constant pressure, A_P is the surface area of the particle, T_∞ is the local temperature of the gas phase, h is the convection heat transfer coefficient, ϵ is the particle emissivity and σ is the Stefan-Boltzmann constant. The convective heat transfer coefficient is calculated via the Nusselt number, as follows:

$$Nu = \frac{hd_p}{k_\infty} = 2 + 0.6Re_d^{1/2}Pr^{1/3} \tag{12}$$

The term d_p is the diameter of the sphere that holds the same volume as the non-spherical particle, Re_d is the Reynolds number based on the particle diameter and relative velocity, and Pr is the Prandtl number of the continuous phase.

Based on the works of Malte & De Bruyn and De Souza, the devolatilization model of choice is the first order model presented in Eq. 13

$$\frac{dm_p(t)}{dt} = -k_v[m_p(t) - m_{p0}(1 - f_{v0})] \tag{13}$$

Where k_v is the chemical kinetic rate calculated via the Arrhenius equation, $m_p(t)$ is the particle mass as a function of time, $m_{p0} = m_p(t = 0)$ and f_{v0} is the volatile mass fraction initially present in the particle.

The surface reaction was modeled by means of the kinetic/diffusion-limited model, where the rate of reaction is determined either by the chemical kinetics or the diffusion rate. The diffusion coefficient and the kinetic rate are determined as follows:

$$D_0 = C_1 \frac{[(T_P + T_\infty/2]^{0.75}}{d_p} \tag{14}$$

$$R = C_1 e^{\frac{-E}{RT_p}} \tag{15}$$

The reaction rate is thus given by:

$$\frac{dm_p(t)}{dt} = -\pi d_p^2 p_{ox} \frac{D_0 R}{D_0 + R} \tag{16}$$

Where T_p is the particle temperature, T_∞ is the local fluid temperature, m_p is the instantaneous particle mass and p_{ox} is the partial pressure of the oxidant species present in the gas phase around the combusting particle.

3.2.5 Fuel properties

The data used to describe the fuel comes from the EBMA biomass characterization laboratory and is presented below, in mass fraction:

Table 1: Fuel parameters.

HCV: 20100 kJ/kg	
Proximate analysis:	**Ultimate analysis:**
Volatile = 0.7210	Carbon (C) = 0.4577
Char = 0.1447	Hydrogen (H) = 0.0647
Ash = 0.0085	Oxygen (O) = 0.4765
Moisture = 0.1258	Nitrogen (N) = 0.001
	Sulphur (S) = 0.0001

From the ultimate analysis of the biomass fuel, we have the chemical formula $C_{3.81}H_{6.42}O_{2.98}N_{0.0071}S_{0.0003}$. From the proximate analysis, one has that 72% of the mass becomes volatiles. Thus, the molecular formula of volatiles is $C_{0.87}H_{2.31}O_{1.07}N_{0.0025}S_{0.0001}$.

For the chemical reaction of volatiles, the two-step reaction mechanism was used. After configuring the solid fuel, the Coal Calculator tool provided the gas phase chemical reaction, as well as the intermediate reaction for CO, shown below.

$$C_{1.11}H_{2.54}O_{0.87}N_{0.0044} + 0.88O_2 \rightarrow 0.86CO + 0.25CO_2 + 1.27H_2O + 0.0022N_2 \tag{17}$$

$$CO + 0.5O_2 \rightarrow CO_2 \tag{18}$$

The heterogeneous surface reaction was considered to be one-step irreversible, as shown:

$$C + O_2 \rightarrow CO_2 \tag{19}$$

3.2.6 Radiation Model

In order to adequately account for the heat transfer due to radiative effects, the P1 model was chosen. It is a simplified case of the general PN model, which is based on the radiation intensity I inside an orthogonal series of harmonic spheres. This model presents several advantages, since it treats the Radiation Transfer Equation (Eq.20) as a diffusion equation, which significantly reduces computational cost. It also works well with geometries that have curvilinear coordinates, such as the cyclonic furnace. This model is the only model that accounts for the heat exchange between particle and gas, besides the Discrete Ordinates model.

$$\frac{dI\left(\vec{r},\vec{s}\right)}{ds} = \alpha\frac{\sigma T^4}{\pi} + \alpha_p\frac{\sigma T_{p,i^4}}{\pi} - \left(\alpha+\alpha_p+\sigma_p\right)I\left(\vec{r},\vec{s}\right) + \frac{\sigma_p}{4\pi}\int_0^{4\pi} I\left(\vec{r},\vec{s}\right)\Phi\left(\vec{s},\vec{s}^{'}\right)d\Omega' \tag{20}$$

Where $\vec{r}$ is the position vector, $\vec{s}$ is the scattering direction vector, s is the trajectory length of the beam, α is the absorption coefficient of the gas phase, α_p is the absorption coefficient of the particle, σ_p is the particle scattering coefficient, σ is the Stefan-Boltzmann constant, I is the radiation intensity, which depends on position and direction, T is the local temperature, Ψ is the phase function and $\Omega^{'}$ is the solid angle.

3.2.7 NOx formation mechanisms

In this work, the thermal (Zeldovich) and fuel NOx mechanisms were used to model the production of the pollutant NO during the combustion. The thermal NOx is generated due to high temperatures and long residence times, and it follows the mechanism proposed by Zeldovich:

$$O + N_2 \overset{k_1}{\longleftrightarrow} N + NO$$
$$N + O_2 \overset{k_2}{\longleftrightarrow} O + NO$$
$$N + OH \overset{k_3}{\longleftrightarrow} H + NO$$

The reaction rates are determined by the following expressions, used by the Fluent package:

$$k_1 = 1.8\cdot 10^8 e^{\left(\frac{-38370}{T}\right)}$$
$$k_{-1} = 3.8\cdot 10^7 e^{\left(\frac{-425}{T}\right)}$$
$$k_2 = 1.8\cdot 10^4 e^{\left(\frac{-4680}{T}\right)}$$
$$k_{-2} = 3.8\cdot 10^3 e^{\left(\frac{-20820}{T}\right)}$$
$$k_3 = 7.1\cdot 10^7 e^{\left(\frac{-450}{T}\right)}$$
$$k_{-3} = 1.7\cdot 10^8 e^{\left(\frac{-24560}{T}\right)}$$

Where k_1, k_2, k_3 are the direct reaction rates; k_{-1}, k_{-2} and k_{-3} are reverse reaction rates. The net production rate of NO is then determined by:

$$\frac{d[NO]}{dt} = k_1[O][N_2] + k_2[N][O_2] + k_3[N][OH] - k_{-1}[NO][N] - k_{-2}[NO][O] - k_{-3}[NO][H] \tag{21}$$

The fuel NOx mechanism deals with the nitrogen present in the biomass particle, and is divided between the nitrogen in the char (N_{char}) and the nitrogen that is liberated during the devolatilization (N_{vol}). The mechanism used in this work follows the pathway presented below:

$$\begin{array}{ccccccc} & & & & N_{char} & & \\ & & & & \uparrow & & \\ N_{volatile} & \longrightarrow & HCN & \xrightarrow{O_2} & NO & \xrightarrow{Char} & N_2 \\ & & \downarrow & & & & \\ & & N_2 & & & & \end{array}$$

As it can be seen, all of the nitrogen present in the char is converted directly into NO, while only the gaseous nitrogen turns into HCN. The source terms defined by the pathway are the following:

$$S_{char,HCN} = 0 \tag{22}$$

$$S_{char,NO} = \frac{S_c Y_{N,char} M_{w,NO}}{M_{w,N} V} \tag{23}$$

Where S_c is the rate of coal consumption in kg/s, $Y_{N,char}$ is the mass fraction of nitrogen in the coal and V is the volume of the cell in m^3.

4. RESULTS

4.1 Velocity

The maximum velocity values obtained were 59.68 m /s, 59.234 m/s and 61.77 m /s for ϕ = 0.35, ϕ = 0.45, ϕ = 0.6, respectively. These maximum speeds are found at the inlet of the mixture in the combustor. The difference between velocities is due to the modification of the global stoichiometric ratio. When we use ϕ = 0.35 the mass of fuel that is entering is smaller than the other two stoichiometric ratios, for the same air flow. It is also possible to note the presence of shear layers between the combustor walls and the central flow.

For the three stoichiometries there is no great differences in relation to the flow behavior. It can be seen in the figures the occurrence of reverse flow near the exit of gases towards the center of the combustor, this mechanism is the main factor for the production of NOx from the thermal mechanism.

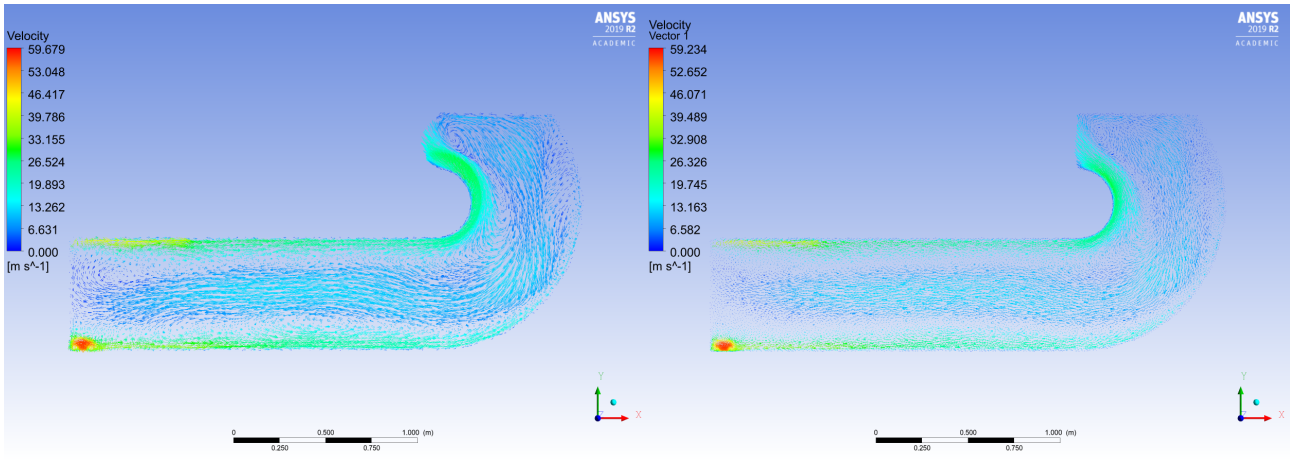

(a) $\phi = 0.3$ (b) $\phi = 0.45$

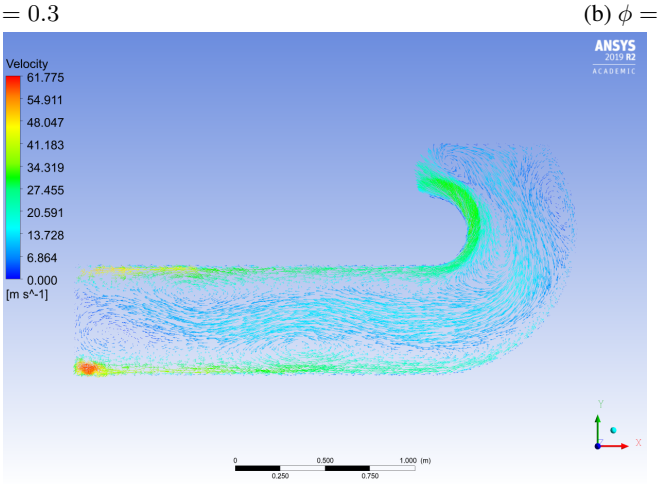

(c) $\phi = 0.6$

Figure 2: Velocity vectors for each case

4.2 Temperature distribution

The temperature distribution in the fig. 6 shows results consistent with those seen in the literature, where the highest temperatures are located in the combustor walls by the cyclonic characteristic of the flow. Temperatures of 1733K, 1735 and 2207K were obtained for the stoichiometric ratios 0.35, 0.45 and 0.6, respectively.

The process of burning of volatiles begins and ends in the initial section of the combustor, approximately $\frac{1}{4}$ of its length, in the temperature range around 1000K. After this initial length range, the increase in temperature was observed due to the volatiles and solids burning at a temperature of approximately 1733 K.

Higher temperatures occur due to the higher volatiles present in the reaction, since these occur with higher stoichiometric ratios, justifying the increase in temperature, mainly with the stoichiometric ratio of 0.6. Also it can be observed that the reaction happens faster.

The transverse plane of temperature distribution is shown in Fig. 5, the region where the combustion reaction occurs is evident. On $\phi = 0.35$ it is possible to highlight the region where the volatiles begin to be released and consumed (green/yellowish coloration) and soon after the solid particles are burnt, where the highest temperatures are identified by the red coloration, the same pattern happens on $\phi = 0.45$ with the volatiles burning shortly before. On $\phi = 0.6$ the process of release and burning of volatiles takes place earlier than that shown in others ratios, so the combustion process occurs faster due to the higher mass of solid.

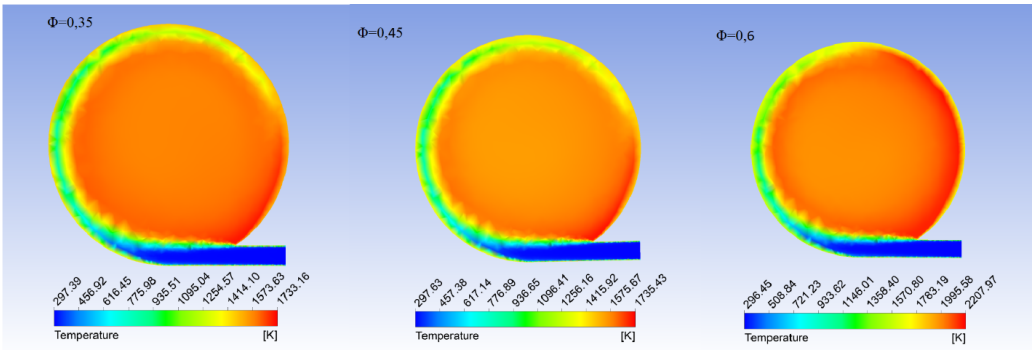

Figure 3: Cross-section of the combustor.

4.3 Species Mass Fraction

4.3.1 Volatiles

Figure 7 shows the mass fraction of the volatiles in relation to the axial distance of the chamber. It can be observed that the consumption of volatiles in the three situations occurs close to 0.5m from the beginning of the combustor. It is important to note that for these equivalence ratios, the air flow is constant with a mass flow rate of 0.1561 kg/s and only the mass flow of the sawdust is modified. For this reason large differences in the lines represented by the ratio of 0.35 (continuous) and 0.45 (dashed with dots) are not noted because the difference in mass flow is not large.

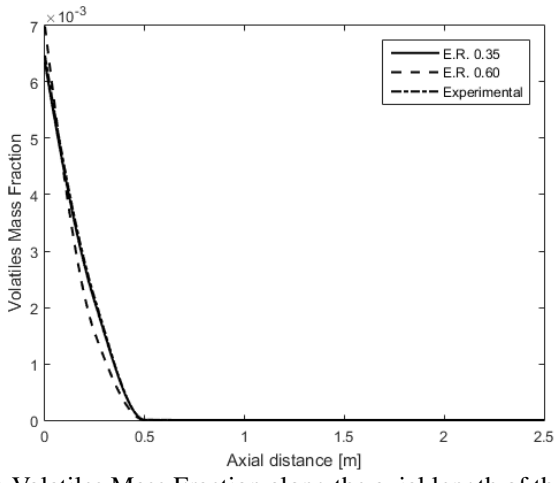

Figure 4: Volatiles Mass Fraction along the axial length of the furnace.

4.3.2 CO_2

In the graph of fig. 8 it is possible to highlight the great difference of CO_2 concentrations of the simulation with equivalence ratio of 0.6 when compared to the others. This is due to higher volatiles, which increases O_2 consumption in the combustion process. It can be said that the equivalence ratio of 0.6 is an excess fuel ratio when compared with the other two, so at the end of the reaction the smoke produced by the combustion gases will be black whereas the ratios of 0.35 and 0.45 are ratios with excess air, will produce lighter smoke.

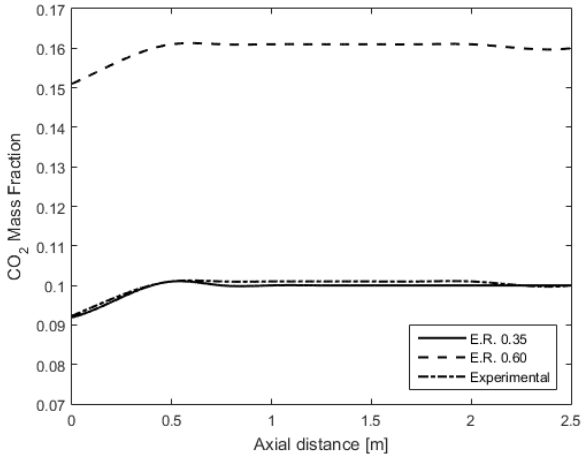

Figure 5:
CO_2 mass Fraction along the axial length of the furnace.

4.3.3 Pollutant NO

As shown in Figs. 3, 4 and 5, gas recirculation occurs near the combustor outlet, this mechanism increases the residence time of the gases in the combustion process, which is the main way to form the NOx pollutant by the thermal mechanism.

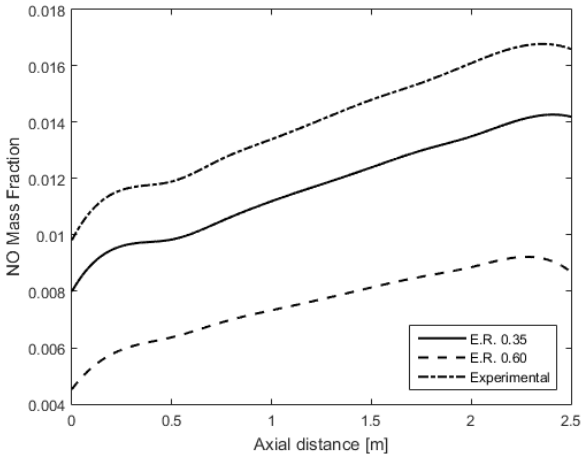

Figure 6: Pollutant NO Mass Fraction along the axial length of the furnace.

Figure 9 shows that NOx formation increases along the reactive tangential flow and has a large increase in the central region of the furnace. Its production is closely linked to the residence time of the combustion reaction product gases at high temperatures inside the furnace. The higher productions of NOx pollutant for stoichiometric is explained by the fact that the reaction equilibrium takes a little longer to be achieved and consequently by the longer residence time of combustion gases, since at the ratio of 0.6 the reaction happens faster and the gases produced spend less time recirculating.

5. CONCLUSION

The development of this work enabled the simulation of reactive biphasic flow, making possible the understanding of the phenomena involved during the combustion reaction in the cyclonic furnace. However, the validation of simulation

results through comparisons with experimental models was not possible due to the limitation of measurement equipment that could provide these experimental results.

From the results of temperature distribution and velocity fields, it can be said that the qualitative behavior of the flow is coherent, and that the quantitative results are within the expected when compared with the literature.

The recirculation phenomenon was observed and its influence on the NOx pollutant generation was analyzed, being evaluated as having a great impact on its generation from the thermal mechanism, since it causes the gases of combustion products to spend more time inside the furnace at high temperature .

The equivalence ratio of 0.45 used in experimental equipment was only used for practicality to operate the chamber, as it has some limitations in the power section. However, as seen in the results, this ratio produces the most NOx pollutants in the reaction product when compared to the 0.6 ratio, which in turn produces a significantly lower amount, since the residence time of the gases is shorter. When compared to the burning of volatiles, no major differences are evident, since all have a fast burning, highlighting the ratio of 0.6 that has a faster burning.

In this study, based on NOx pollutant production and volatile flaring, the ratio that showed the best was 0.6. Further studies should be done, such as determining the furnace thermal efficiency and the furnace burning efficiency to make the study even more conclusive.

Regarding to the development of the combustion reaction, it was observed that in the conditions evaluated, the reactions occurred completely after 0.35 cm to 0.50 cm of the length of the furnace from its feeding, allowing the domain decrease, making the equipment more compact

6. REFERENCES

Almeida, Ana and S. Vieira, Mônica and Ribeiro, Albina and Pereira, Isabel and P. Neto, Maria and M. Pilão, Rosa. 2016. Effect of Air/Biomass Ratio on the Gasification of Olive Bagasse Particles. International Journal of Environmental Science and Development. 7. 269-272. 10.7763/IJESD.2016.V7.782.

ANSYS, 2011. ANSYS FLUENT Theory Guide. 14.0 ed. s.l.:s.n.

ANSYS, 2012. ANSYS FLUENT Meshing User Guide. s.l.:s.n.

Cunha, F. A., 2005. Análise experiemental e simulação nemérica da combustão de serragem em um combustor ciclônico. 143f. Dissertação (Mestrado em engenharia mecânica) - Universidade Federal do Pará.

Guessab, A. A. A. B., 2013. Simulation of turbulent piloted methane non-premixed flame based on combination of finite-rate/eddy-dissipation model. MECHANIKA.

Lima, Rodrigo Cavalcanti. 2016. Estudo da simulação da combustão de pó de biomassa em uma fornalha ciclônica. Dissertação (Mestrado em engenharia mecânica) - Universidade Federal do Pará.

Silva, C.V., França, F.H.R., Vielmo, H.A., 2007.Analysis of the turbulent, non-premixed combustion of natural gas in a cylindrical chamber with and without thermal radiation. Combustion Science and Technology, Vol. 179, pp.1605-1630.

Silva, C. V., Indrusiak, M. L. S. and Beskow, A. B., 2019. CFD Analysis of the Combustion Process in a Boiler of a 160 MWe Power Plant: Leakage Influence . Journal of the Brazilian Soc. Mechanical Sciences.

Tillman, David A. 1991. The Combustion of solid fuels and wastes. Academic Press, San Diego, U.S.A., 1991. 378 pp.

Turns, S. R. 2012. An Introduction to Combustion: Concepts and Applications. New York: McGraw-Hill.

Vasconcelos, A. K. 2008. Influencia da variação da razão de alimentação ar/serragem de um combustor ciclonico na composição de seus produtos gasosos. 114f. Dissertação (Mestrado em engenharia mecânica) - Universidade Federal do Pará.

Versteeg, H. K. Malalasekera, W., 2007. An Introduction to Computational Fluid Dynamics: The Finite Volume Method.. 2^a ed. s.l.:Pearson Education Limited.

Wenjing S, Wenqi Z, Aibing Y, Longhai L, Yujun Q. Numerical investigation on the flow, combustion and NOx emission characteristics in a 660 MWe tangential firing ultra-supercritical boiler. Advances in Mechanical Engineering, 2015: 8(2): 1 - 13.

Yin, C., 2015. On gas and particle radiation in pulverized fuel combustion furnaces. Applied Energy.

7. RESPONSIBILITY NOTICE

The author(s) is (are) the only responsible for the printed material included in this paper.